Experiments on feedback control of multiple resistive wall modes comparing different active coil arrays and sensor types

J.R. Drake[1], P.R. Brunsell[1], D. Yadikin[1], H. Bergsåker[1], M. Cecconello[1], A. Hedqvist[2], M. Kuldkepp[2], S. Menmuir[2], E. Rachlew[2]

1) Division of Fusion Plasma Physics, Alfvén Laboratory, Association EURATOM-VR, School of Electrical Engineering, Royal Institute of Technology KTH, Stockholm, Sweden
2) Department of Physics, Association EURATOM-VR, School of Engineering Science, Royal Institute of Technology KTH, Stockholm, Sweden
e-mail contact of main author: james.drake@ee.kth.se

Abstract. Experiments have been carried out on the EXTRAP T2R reversed-field pinch device to study several important issues related to feedback control of resistive wall modes (RWMs). The feedback system includes a sensor coil array, a feedback controller implementing a feedback law and an active coil array. The issues include 1) effects of sideband harmonics produced by the feedback system, 2) the form of the controller and the feedback law, 3) feedback system stability, 4) selection of the sensor coil configuration and 5) effects of field errors on the feedback system. Side band harmonics are produced by the feedback system because the active saddle coil array consists of discrete coils. The presence of side bands can couple modes thus preventing simultaneous stabilisation of the coupled modes. The side band effect sets requirements for the minimum number of active coils in the array in both the poloidal and toroidal directions. Recent experiments using the intelligent shell concept with proportional-integral-derivative controller action have achieved complete simultaneous stabilisation of all RWMs modes when the requirements are satisfied. In addition to the intelligent shell concept, preliminary experiments have been performed to test the fake rotating shell concept. For this concept, the sensor coil array is shifted in phase relative to the active coil array thus a detected harmonic is induced to rotate by the active coil-produced control field. Under the condition that the phase shift is less than a quarter-wave length of the mode, mode suppression can be achieved. Feedback using a controller incorporating individual mode control has also been tested. This has enabled the first feedback experiments using a sensor array measuring the toroidal field component to be carried out. For this concept, an array consisting of localised toroidal field sensor coils is used. Mode suppression has been successfully accomplished. However pick-up of high order field error harmonics due to the small size of the sensor coils introduces an adverse signal to background ratio as compared to the case with the radial field sensor coil array. Optimal suppression is achieved at the predicted complex feedback gain phase. Mode rotation is induced at other complex gain phases, in agreement with modelling. In other experiments, linear models have been used to evaluate the effect of resonant field errors on mode growth. The thin-wall model is satisfactory for describing the response of the plasma and resistive-shell system and resonant field error amplification is observed.

1. Introduction

Feedback control of resistive wall modes is of common interest for toroidal fusion concepts that use conducting walls for stabilization of ideal MHD modes. According to the thin-wall model if the wall is resistive and lies within the position for ideal wall stabilization, a class of modes called resistive wall modes (RWMs) develop with growth rates of the order of the wall penetration time [1]. For the advanced tokamak, control of modes with low toroidal mode number n is of primary interest for achieving beta above the no-wall limit (RWMs are $n \neq 0$ pressure-driven external kinks). For the reversed-field pinch (RFP), there are unstable modes with poloidal mode number $m = 1$ with a range of toroidal mode numbers which must be simultaneously controlled.

The commonly used feedback control system includes a sensor consisting of an array of magnetic coils (measuring mode harmonics), an actuator consisting of an array of active saddle coils (producing control harmonics) and a controller that implements a feedback law in real time. Active feedback control of RWMs has previously been demonstrated on the EXTRAP T2R reversed-field pinch experiment [2-4]. These experiments have shown that, for the purposes of modelling the feedback system, the mode growth is adequately described by linear MHD theory. However there are a number of issues that must be considered when designing and optimising a RWM feedback system and these issues lead to requirements and constraints on the sensor coil array, the active coil array and the feedback law that make up the feedback system. Issues that have been studied on the EXTRAP T2R device include the following:

- The effect of sideband harmonics generated by the actuator coil array due to the finite number of coils in the array.
- Selection of the feedback concept; for example intelligent shell [5], so called fake rotating shell [6, 7], or individual mode feedback with real or complex gain [8].
- Feedback system stability considerations; for example required gain and inclusion of proportional and/or integral or derivative components.
- Selection of sensor array; for example measurement of radial field (perpendicular to wall) or toroidal field (tangential to wall).
- Effect of intrinsic field errors on the performance of the feedback system.

In this paper the results of experiments focusing on these issues are described. EXTRAP T2R is suitable for studies of RWM control for several reasons: 1) the simple geometry (circular cross-section, large aspect ratio) enables the use of a cylindrical model, 2) the dominant modes are helical harmonics, characterised by poloidal and toroidal mode numbers, 3) the modes are driven by the equilibrium current density gradient and therefore the stability is easily parameterised both in experiment and theory, 4) the modes are non-resonant and their stability is not affected by sub-Alfvénic plasma rotation, 5) the observed RWM growth is reproducible, both in terms of phase and amplitude.

The general spatial dependence for a RWM harmonic at the minor radius of the sensor coil array is given by $b_{n,sens}(\theta,\varphi) = b_n^0 \exp[i(m\theta + n\phi)]$ where b_n^0 is the mode amplitude and m and n are the poloidal and toroidal mode numbers (only $m = 1$ is considered for the RFP case in the following discussion). Experimentally the harmonic is derived from a real-time fast Fourier transform (FFT) of the measured sensor coil array signals. The mode harmonic is multiplied by a gain that can be complex, $G_n = |G_n| \exp(i\alpha_n)$, which gives the desired control harmonic. Applying an inverse FFT then gives the distribution and amplitude of currents that are to be produced in the active coils. The feedback loop action is repeated with a rate dependent on the latency-time of the controller.

A general issue for RWM feedback systems is the coupling of modes introduced by the generation of side bands in the magnetic field mode spectrum produced by the active array. The actuator coil system has a discrete number of coils in the poloidal direction (M_c) and toroidal direction (N_c). The separation of the side band harmonics, in terms of mode number, is dependent on the number of coils in the array. The side band harmonics can couple the growth of unstable modes or stimulate the growth of marginally stable harmonics through field error amplification [9, 10].

A basic control method is the intelligent shell concept, which minimizes the total signal in a radial field sensor at the wall. In order to optimise the feedback, the controller can incorporate a feedback law to determine the gain that includes components based on the integral or derivative sensor signals as well as the component that is proportional to the sensor signal. The fake rotating shell in effect incorporates a complex feedback gain, essentially adding a phase shift to the control field, thereby inducing rotation of the modes.

The generic feature of a RWM is magnetic diffusion of the non-axisymmetric mode in the thin wall. Therefore, flux loops measuring the local perpendicular component of the magnetic field (radial component in cylindrical co-ordinates) at the wall are typically used as sensors. However sensors that measure the tangential field inside the wall have also been suggested. This concept requires resolution of the RWM perturbation into harmonics and feedback action on individual modes. The potential advantage of tangential sensors is that the coupling is reduced between the active saddle coils that produce the control field at the wall and the sensor array [8].

2. The EXTRAP T2R reversed-field pinch

The EXTRAP T2R device is a reversed-field pinch with a resistive shell (or wall) and is described in detail in reference [11]. The resistive shell has a magnetic penetration time for an $n = 0$ vertical field of $\tau_w = 6.3$ ms. The spectrum of $m = 1$ RWMs is shown in FIG. 1. The unstable RWMs have $m = 1$ and are mainly non-resonant; there is no flux surface with a safety factor $q = 1/|n|$ where n corresponds to an unstable RWM. By convention, modes with a handedness corresponding to the pitch of field lines inside the reversal surface have $n < 0$ and modes outside the reversal surface have $n > 0$. The system for active control of RWMs installed on T2R includes a full-coverage, radial-field coil array located just inside the shell that consists of 64 (toroidal) by 4 (poloidal) positions of which 32 toroidal positions are used in the sensor coil array, and a full-coverage saddle coil array located just outside the shell that is 32 (toroidal) by 4 (poloidal). The saddle coil width is twice the sensor coil width. Control harmonics can be produced for targeted $m = 1$ modes in the range $-16 \leq n \leq 15$ with side bands at $\Delta n_{sb} = 32$ intervals. The saddle coils are powered by suitably modified audio amplifiers.

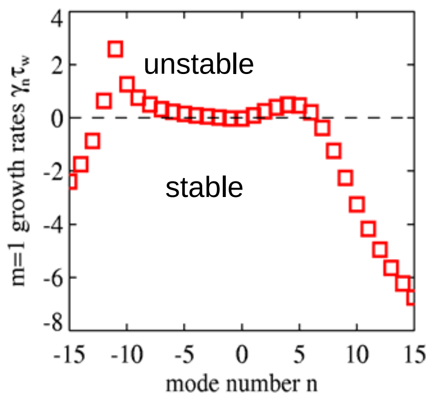

FIG.1. Spectrum of m=1 modes in the EXTRAP T2R device. The unstable modes are -11≤n≤-2 (internally non-resonant) and 1≤n≤6 (externally non-resonant). Modes n ≤ -12 are resonant.

The digital feedback controller used on T2R is a prototype of the controller developed for the RFX device at Padova [12]. The controller can be operated as an intelligent shell controller, with full PID action, and as an individual mode controller, where the feedback law that is implemented potentially has a different complex gain for each resolved harmonic.

3. Side band effect

The active coil array consists of a discrete number of coils. In EXTRAP T2R, the chamber cross-section is circular and there is full coverage of the shell with $M_c = 4$, and $N_c = 32$. If the controller targets a specific mode (m_o, n_o), then side bands are produced at $m_{sb} = m_o \pm kM_c$ and $n_{sb} = n_o \pm lN_c$ where $k,l = 1,2,3,\ldots$. Concerning the negative effects of side bands, in experiments it has been shown that if $M_c = 4$, the sideband effect due to the discrete number of coils in the poloidal direction can be neglected. For $m = \pm 1$, the closest sidebands are then at m_{sb}= -5, -3, 3 and 5, and all such modes are robustly stable. However, the number of coils in the toroidal direction N_c must be sufficient so that the side bands for all unstable modes correspond to robustly stable modes. For example, for the $n = -10$ mode, with $N_c = 32$, the first side bands are at $n_{sb} = -42$ and $n_{sb} = 22$. Both of these modes are robustly stable, as seen in FIG. 1. However if the number of toroidal positions is reduced to $N_c = 16$, unstable modes are coupled by the side band effect. For example the $n = -10$ and $n = 6$ modes, which are both unstable, are coupled and cannot be stabilised simultaneously with intelligent shell feedback. Experimental studies of this effect are described in detail in References [2-4].

This effect is demonstrated in FIG. 2 which shows the effect of feedback using an active coil array with M_c = 4 and $N_c = 16$. Comparing panels (a) and (b) it is seen that without feedback, both the $n = -10$ and $n = 6$ modes have growing amplitudes, but the $n = -10$ mode has a larger amplitude as expected (see FIG. 1). With feedback using the 4x16 configuration, the controller produces a harmonic to suppress the $n = -10$ mode, but the side band reinforces the n = 6 mode growth. The $n = -10$ mode is dominant, so the sideband effect of the n = -10 mode on the n = 6 mode dominates over the sideband effect of the n = 6 mode on the n = -10 mode. The end result is a partial suppression of the n = -10 mode and faster growth of the $n = 6$ mode [13].

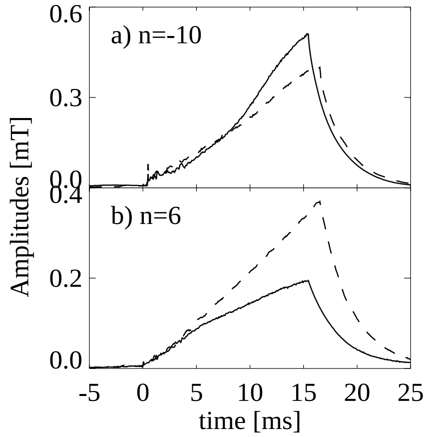

FIG. 2. The time dependence of mode harmonic amplitudes without feedback (solid line), with feedback using the 4x16 active coil configuration (dotted line); (a) m=1, n=-10. (b) m=1, n=6.

New experiments have been performed with N_c = 32 but with only 2 coils in the poloidal direction, M_c = 2. The toroidal sideband interval is Δn_{sb} = 32 and these sidebands are unimportant. The poloidal sideband effect however becomes important because with M_c = 2, the m = -1 and m = 1 modes having the same n are coupled. The amplitude of a perturbation with mode numbers (1, n) is $A_{1,n}^2 = b_{1,n} \cdot b_{1,n}^*$, where $b_{1,n}$ are complex Fourier coefficients. The perturbations are real so that $b_{1,n}^* = b_{-1,-n}$. If the controller produces a control harmonic for mode numbers (m, n) = (1, n) then a side band harmonic, (-1, n), is produced with amplitude $A_{-1,n}^2 = b_{-1,n} \cdot b_{-1,n}^*$. Using the relations $b_{-1,n} = b_{1,-n}^*$ and $b_{-1,n}^* = b_{1,-n}$ then gives an expression for the amplitudes of the coupled modes $A_{-1,n}^2 = A_{1,-n}^2$. The effect can be summarised by saying that four equally spaced coils in the poloidal direction can produce both the sine and cosine components of the perturbation, but two equally spaced coils produce only one of the components. In FIG. 3, a spectrum is shown for a vacuum case where the digital controller is programmed to produce the (m, n) = (1, 6) harmonic. A side band of equal amplitude is produced for $n = -6$. The effect of the toroidal side bands on plasma mode growth is shown in FIG. 4. Without feedback, both the $n = 6$ and $n = -6$ modes are observed, but the unstable $n = 6$ mode has a larger amplitude than the marginally unstable n = -6 mode. With feedback using the 2x32 configuration, the controller produces a harmonic to suppress the n = 6 mode, but the side band reinforces the $n = -6$ mode growth. The end result is that the n = 6 and n = -6 modes are coupled and their growth is not suppressed. Furthermore, they have about the same amplitude with a phase difference of π as predicted [4, 13].

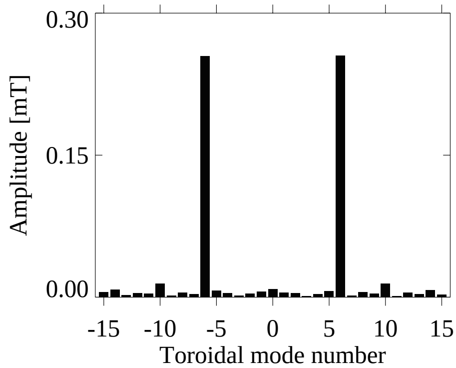

FIG. 3. The vacuum |m|=1 mode spectrum for a targeted mode n=6 for the active coil configuration with M_c=2 and N_c= 32.

4. Intelligent shell

For EXTRAP T2R, full coverage with M_c=4 and N_c=32 is sufficient for stabilisation of all the unstable RWMs in the spectrum shown in FIG. 1. A series of experiments has been performed with the full coverage active coil system to study the requirements for stabilisation of all the unstable modes with intelligent shell feedback. The original intelligent shell feedback system as envisioned by Bishop [5] incorporates discrete active coils and overlapping sensor coils that measure the perpendicular component of the non-axisymmetric growing modes. In the most basic form of the intelligent shell scheme, it is not necessary to resolve the mode spectrum. Each active coil and coincident sensor coil form a subsystem. The feedback law is simply to zero the sensor signal, b_{sens}. The control field is $b_{cont}= -Gb_{sens}$, where G is real. On T2R, the digital controller can also be used in the intelligent shell configuration with a one-to-one relation of sensor and active coil. The latency time in this configuration is less than for the mode control configuration. Also, in recent experiments full PID controller action is incorporated. Complete stabilisation of the modes is achieved. An example of a plasma discharge without feedback and with intelligent shell feedback is shown in FIG. 5. The amplitudes of representative RWMs are shown. Without feedback, the RWMs grow on a time scale in agreement with the normalised growth rates shown in FIG. 1. The discharge shown in FIG. 5 terminates after three wall times.

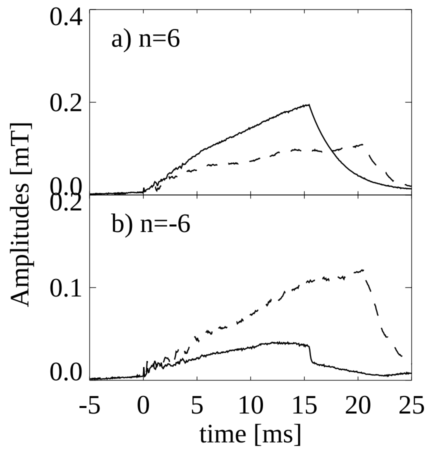

FIG. 4. The time dependence of mode harmonic amplitudes without feedback (solid line), with feedback using the 2x32 active coil configuration (dashed line); (a) |m|=1, n=6. (b) |m|=1, n=-6.

With feedback, growth of the unstable modes is suppressed, and the pulse length is ten wall times. The limitation is set by the power supplies.

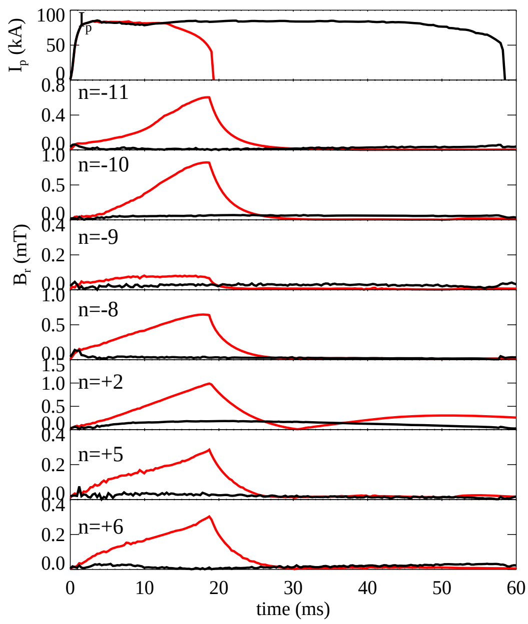

FIG. 5. Comparison of discharges with and w/o feedback control. The panels are as follows: plasma current, modes m=1, n=-11, -10, -9, -8, +2, +5, +6.

5. Fake rotating shell

The concept called fake rotating shell has been tested on EXTRAP T2R [14]. The full sensor coil array for the radial field has 64 toroidal positions, which means that the sensor coil center-to-center separation is $\delta\varphi_s=\pi/32$ radians. The separation of the active coils is $\delta\varphi_a = \pi/16$. Therefore by running the controller in the intelligent shell mode but with the sensor array connections displaced by $\delta\varphi = \pi/32$, the mode harmonics produced by the active coils will be displaced by $\delta\varphi = \pi/32$ relative to the harmonics derived from the sensor coil signals. Since the displacement is fixed, the phase shift of the control harmonic relative to the plasma harmonic will be dependent on the toroidal projection of the wave length of the mode, $\delta\varphi_n = 2\pi/n$. For the fake rotating shell to be effective, the displacement $\delta\varphi = \pi/32$ should be less than $\delta\varphi_n/4$, which corresponds to the condition that $|n| < 16$ for the fake rotating shell to have a stabilising effect for the EXTRAP T2R device. The results of a fake rotating shell test experiment are shown in FIG. 6. Amplitudes are shown for the modes with $n = \pm5$, ($|n| < 16$), and for $n = \pm20$, ($|n| > 16$) as well as for $n = -14$. The low–n modes are non-resonant RWMs and their growth is suppressed. The $n = 20$ mode is robustly stable RWM, but the mode amplitude is increased indicating that the fake rotating shell can potentially destabilise modes if the phase shift of the control harmonic is greater than a quarter wave length of the mode. Indeed the pulse discharge length is shorter with fake rotating shell feedback. The $n = -14$ mode and the $n = -20$ mode are resonant tearing modes. These tearing modes normally exhibit natural rotation, induced by the plasma rotation, and have velocities far exceeding the inverse wall time. As a result the radial fields at the wall for these harmonics are normally low unless the modes wall lock. The action of the fake rotating shell induces wall locking for the n = -20 mode, however the effect on the n=-14 mode is initially small.

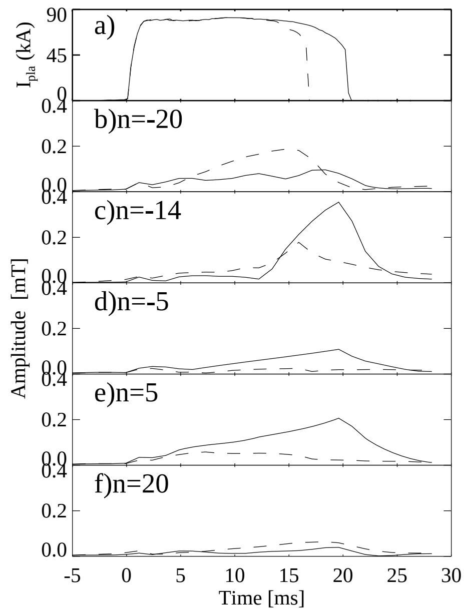

FIG. 6. Mode growth without feedback (solid line) and with fake rotating shell feedback (dashed line). (a) plasma current. (b) n=-20. (c) n=-14. (d) n=-5. (e) n= 5. (f) n=20.

6. Feedback system stability

Studies of the gain required to achieve full stabilisation of the modes in the intelligent shell configuration have been performed and are described in detail in Ref. [13]. An advantage of the intelligent shell configuration, with a shorter latency time, is that higher gains can be implemented while maintaining feedback system stability. Also, comparisons have been made between controllers with only proportional feedback and controllers with proportional plus different combinations of integral and derivative gain coefficients. The studies demonstrate that for the EXTRAP T2R feedback system there is a smooth improvement of mode suppression with increasing gain and there is a range of gain values for which adequate suppression can be achieved with proportional gain. Introduction of integral gain reduces the required proportional gain for mode suppression. For gains larger than that required for suppression of mode growth, the mode amplitude starts to oscillate. Incorporation of a derivative gain suppresses the tendency for oscillation allowing full suppression. In summary, for the EXTRAP T2R device and controller, there is a stable feedback system operation range where mode suppression is achieved for many wall times as seen in FIG.5.

Experiments using the individual mode feedback concept have also been carried out. The digital controller utilises a real time Fourier transform of sensor data, and therefore has a longer latency time. The studies show that the growth of the dominant RWMs can be simultaneously suppressed with about the same gain requirements as for the intelligent shell concept without integral and derivative feedback action, however the system stability limit is at a lower gain level [15].

7. Sensor coil configuration

Using the individual mode control configuration, the feedback gain can be set for selected harmonics, with both real and complex values (targeted-harmonics). Using the mode control concept, it has been possible to carry out the first feedback experiments using a sensor array measuring a tangential field component at the wall (toroidal field) [13]. The results have been compared with mode suppression achieved with radial field sensors. According to theory, the gain required for suppression of the RWM instabilities can be lower for the case with sensors measuring a tangential component of the perturbation (toroidal component) as compared to a system with sensors measuring the perpendicular component of the perturbation (radial component) [8]. A mode control scheme with complex feedback gain is used, targeting one dominant mode (m = 1, n = -11). As seen in FIG. 7 mode suppression is achieved. The phase shift of the control field has been varied. The best suppression is achieved at the predicted complex feedback gain phase around π/2. Mode rotation is induced at other complex gain phases. In these experiments suppression is seen when targeting individual modes. However simultaneous suppression of all modes has not yet been achieved. This is attributed to the fact that the toroidal sensors are small in size and therefore are sensitive to pickup of high order field error harmonics that are ubiquitous due to structural features. The dimensions of the radial field pick up coils are sufficiently large so that pick up of high order field errors is lower. In general it is anticipated that the use of the tangential component will require more signal conditioning of the sensor coil data. This is an area for future studies.

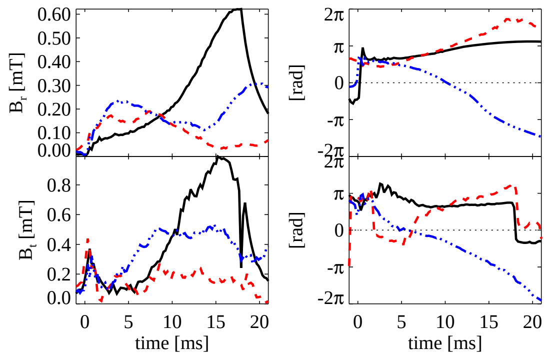

FIG. 7 Feedback using toroidal field sensors. Mode control scheme targeting m=1, n=-11. Variation of the complex feedback gain phase. Radial (top) and toroidal (bottom) field at wall. Left: Mode amplitudes, Right: Mode phases. Traces are shown for reference shot without feedback (full), feedback with complex gain phase π/2 (dashed), feedback with gain phase 5π/6 (dot-dashed).

3. Field error effects

Open loop experiments have been used to observe the effects of resonant field errors applied to unstable, marginally stable and robustly stable modes [10]. The observed effects of field errors are consistent with the thin-wall model, where growth of the mode perturbation for the (m, n) harmonic is determined by the resonant field error amplitude ($b^{err}_{m,n}$), the wall penetration time for the harmonic ($\tau^{w}_{m,n}$) and the growth rate of the harmonic ($\gamma_{m,n}$). The equation for the growth of the harmonic is given by [4, 9],

$$\tau^{w}_{m,n}\frac{db_{m,n}}{dt} = b^{err}_{m,n} + \gamma_{m,n}\tau^{w}_{m,n}b_{m,n}. \qquad (1)$$

The wall penetration time and growth rate are mode-number dependent and have been experimentally measured with good accuracy for the EXTRAP T2R device for a range of modes [10]. An analysis based on Eq. (1) was performed to demonstrate that the effect of field errors can be incorporated into the linear MHD model describing mode growth. As seen in Eq. (1), the growth of the mode has two components; the first term depends on the field error harmonic and the second term depends on the growth rate. There is always a non-zero field error present for every harmonic. A localized field error due to a structural element introduces a broad band of harmonics. The terms $\tau^{w}_{m,n}$ and $\gamma_{m,n}$ in Eq. (1) are known and therefore the amplitude of the field error harmonic can be derived from the observed mode growth. An example of a study is shown in FIG. 8. Three modes are selected; two unstable modes, n = -10 and n = 5, where the mode growth is dominated by the instability term and one marginally stable mode, n = 2, where the mode growth is dominated by a resonant field error term. The amplitudes of the field error harmonics calculated from Eq. (1) are also shown. Note that the growth of the marginally stable mode that is stimulated by the field error is an example of resonant field error amplification.

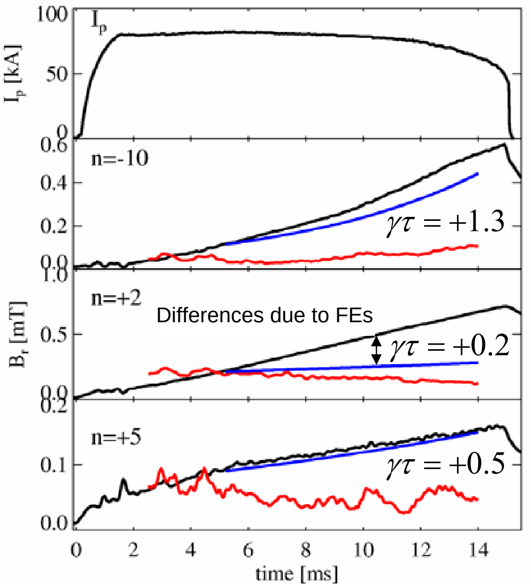

FIG. 8. The growth of three modes is analysed to determine the amplitude of the resonant field error. The black trace is the observed mode growth, the blue trace is the calculated growth from the amplitude at 5 ms and the known growth rate, and the red trace is the calculated field error amplitude based on Eq. (1)

8. Conclusion

Important issues for optimisation of RWM active feedback systems have been studied in the EXTRAP T2R reversed-field pinch. An important basic result is that the thin-wall linear MHD stability analysis model for the determination of the mode stability and the description of the plasma thin-wall system can be successfully used in an analysis of a feedback system. Furthermore, stabilisation of the full range of modes can be achieved. There are requirements on the system that must be considered. These include an adequate number of coils in the array to avoid coupling unstable or marginally stable modes with the ubiquitous side-band effect. Advanced feedback systems such as the fake rotating shell and use of tangential components in the sensor array have been tested with encouraging results.

References

[1] C.G. GIMBLETT, Nucl. Fusion **26** (1986) 617.
[2] P.R. BRUNSELL, D. YADIKIN, D. GREGORATTO, *et al*, Phys rev. Lett. 93 (2004) 225001.
[3] J. R. DRAKE, P.R. BRUNSELL, D. YADIKIN, *et al*, Nucl. Fusion **45** (2005) 557.
[4] P.R. BRUNSELL, Plasma Physics and Controlled Fusion **47** (2005) B25-B36 Sp. Iss SI Suppl.12B.
[5] C.M. BISHOP, Plasma Phys. and Controlled Fusion **31**, 1989) 1179.
[6] C.G. GIMBLETT, Plasma Phys. Controlled Fusion **31** (1989) 2183.
[7] R. FITZPATRICK and T.H. Jensen, Phys. Plasmas **3** (1996) 2641.
[8] R. PACCAGNELLA, D. GREGORATTO, A. BONDESSON, Nucl. Fusion 42, (2002) 1102.
[9] V.D. PUSTOVITOV, Fizika Plazmy **30** (2004) 211.
[10] D. GREGORATTO, J.R. DRAKE, *et al*, Phys. of Plasmas **12** (2005) Art. No. 092510.
[11] P.R. BRUNSELL, *et al.*, Phys. of Plasmas **10** (2003) 3823.
[12] M. CAVINATO, *et al*, "Comparison of strategies and regulator design for active control of MHD modes", 23rd Symposium on Fusion Technology, 20-24 September 2004, Venice Italy, Paper P3C-C-377.
[13] D. YADIKIN, P. R. BRUNSELL and J.R. DRAKE, Plasma Physics and Controlled Fusion **48** (2006) 1.
[14] D. YADIKIN, P. R. BRUNSELL and R. PACCAGNELLA, Phys. of Plasmas 13 (2006) Art No. 072109.
[15] P.R. BRUNSELL, et al, "Reversed-field pinch operation with intelligent shell feedback control in EXTRAP T2R" to be published in Nucl. Fusion.